Cytometry 13:571–576 (1992)

Quantification by Laser Scan Microscopy of Intracellular Doxorubicin Distribution[1]

J.H.M. de Lange, N.W. Schipper, G.J. Schuurhuis, T.K. ten Kate, Th.H.M. van Heijningen, H.M. Pinedo, J. Lankelma, and J.P.A. Baak[2]

Departments of Pathology (J.H.M. de L., N.W.S., T.K.t.K., J.P.A.B.), Medical Oncology (G.J.S., Th.H.M.V.H., H.M.P., J.L.), Free University Hospital and Netherlands Cancer Institute (H.M.P.), Amsterdam, The Netherlands.

Received for publication October 4, 1990; accepted December 13, 1992.

Changes in intracellular drug localization accompany doxorubicin resistance in multidrug resistant tumor cells. The purpose of this study was to develop a method to quantify these changes and so detect different levels of resistance. Tumor cells were incubated with the fluorescent anthracycline doxorubicin (excitation at 480 nm; emission maximum at 560–590 nm) and were quantified using laser scanning microscopy. The fluorescent mode was used to record the intracellular drug distribution, whereas the absorption mode was used to define the nuclear and cytoplasmic boundaries. The cell compartments were delineated interactively on an image processing system and the ratio nuclear fluorescence/cytoplasmic fluorescence (N/C ratio) was determined. N/C ratios were: 1.8 in the Chinese hamster ovarian cell line AUXB1 and 0.1 in its MDR subline CH^RC5; 3.8 in the human squamous lung cancer cell line SW-1573 and 1.8 and 0.4 in its MDR sublines SW-1573/2R120 and SW-1573/2R160, respectively; and 3.6 in the human myeloma cell line 8226/S and 2.1 and 1.0 in its MDR sublines 8226/Dox4 and 8226/Dox40, respectively.

The doxorubicin distribution was independent of the doxorubicin concentration within a range from 1–32 μM. Furthermore, the progressive mean of the nuclear/cytoplasmic doxorubicin fluorescence ratio showed that a minimal sample size of 30 cells is necessary for reliable results. The results of two independent assessments showed a high reproducibility (r = 0.97). Thus, with the method described in this paper, it is possible to detect relatively low levels of doxorubicin resistance (factor 8).

Key terms: Multidrug resistance, doxorubicin distribution, laser scan microscopy, digital image processing

The development of drug resistance is a major problem in cancer chemotherapy (7). Multidrug resistance (MDR) is characterized by a broad cross-resistance to natural compounds, such as anthracyclines (e.g., doxorubicin) and Vinca alkaloids (7) and decreased cellular drug accumulation, because of increased efflux of the drug via P-glycoprotein (for an overview see (7)).

For anthracyclines in MDR cells, it has been found that, in addition to a decrease in the drug accumulation, the intracellular distribution of the drug is changed in human myeloma (2), myeloid (6), and lung tumor cells (8), in Chinese hamster ovarian and human ovarian carcinoma cells (11), and in epidermoid carcinoma cells (14). Anthracycline fluorescence is found mainly in the nucleus in sensitive cells and mainly in the cytoplasm in cells with a relatively high level of resistance (2,8,11,14). However, most studies thus far were only qualitative. In order to estimate the contribution of such differences in drug distribution to drug resistance (especially the low and clinically more rele-

[1]This work was supported in part by grants from the Praeventiefonds (grant #28/834), from the Netherlands Cancer Foundation (IKA VU 88-22), and the Bristol-Myers Squibb Company.

[2]Address reprint requests to Dr. J.P.A. Baak, Dept. of Quantitative Pathology, Free University Hospital, De Boelelaan 1117, 1007 MB Amsterdam, The Netherlands.

Abbreviations: HEPES, 4-(2-hydroxyethyl)-1-piperazineethane sulphonic acid; MDR, multidrug resistance/resistant; N.A., numerical aperture; N/C ratio, nuclear/cytoplasmic doxorubicin fluorescence ratio; PBS, phosphate-buffered saline, pH 7.4.

vant levels), quantitative techniques are needed. Laser scan microscopy is an appropriate technique since it offers the opportunity to detect the weak fluorescence of the anthracycline doxorubicin in sensitive and resistant cells. At the same time the nature of the method, i.e., scanning the object, results in minimal fading (1,13).

In this work, the image acquisition with laser scan microscopy, as well as the procedure for the interactive measurements established by digital image processing, are described and evaluated. As for the image acquisition, special attention has been paid to the effect of the laser beam on the fluorescence in living nonfixed cells. As for the image analysis, the focus has been on the sample size needed for reliable results, the reproducibility of the assessments, and the detection of different resistance levels by using the ratio nuclear doxorubicin fluorescence to cytoplasmic doxorubicin fluorescence (N/C ratio).

MATERIALS AND METHODS

Cell Preparation

This study used the Chinese hamster ovarian cell line AUXB1 and its colchicine-resistant subline CH^RC5 (10), the human squamous lung cancer cell line SW-1573 and its doxorubicin-resistant sublines SW-1573/2R120 and SW-1573/2R160 (9), and the human myeloma cell line 8226/S and its doxorubicin-resistant sublines 8226/Dox4 and 8226/Dox40 (4).

Cells were cultured in plastic flasks (A/S Nunc, Roskilde, Denmark) in a humidified atmosphere at 5% CO_2. SW-1573 and 8226 cells were maintained in Dulbecco's modified Eagles medium (Gibco, Europe Ltd., Paisley, Scotland) supplemented with glutamine containing 7.5% fetal bovine serum (Flow Laboratories, Irvine, U.K.). The Chinese hamster ovarian cell lines were cultured in MEM Alpha Medium (Gibco).

The resistant cell lines were cultured in the presence of drugs; 10 μg/ml colchicine for the CH^RC5 cell line, 120 and 160 nM doxorubicin (Farmitalia Carlo Erba S.A., Nivelles, Belgium) for the SW-1573/2R120 and SW-1573/2R160 cell lines, respectively, and 40 and 400 nM doxorubicin for the 8226/Dox4 and 8226/Dox40 cell lines, respectively. The levels of resistance to doxorubicin are 350 (CH^RC5), 11 (SW-1573/2R120), 45 (SW-1573/2R160), 8 (8226/Dox4), and 50 (8226/Dox40).

For the fluorescence experiments, adherent Chinese hamster ovarian cell lines and human squamous lung cancer cells were detached using a solution containing 0.025 mg/ml trypsin and 2.5 mg/ml EDTA in Ca^{++} and MG^{++}-free Hanks' buffered salt solution, plated in tissue culture disks with a density of $0.5.10^6$ cells per well (diameter: 32 mm, Costar, Cambridge, MA) and after 18–24 h incubated with doxorubicin for 2 h in $NaHCO_3$-free cell culture medium, containing 20 mM HEPES buffer, pH 7.4 at 37°C.

The human myeloma cells (suspension cells) were allowed to attach to wells with a density of $0.5.10^6$ cells per well during 30 min at 4°C in serum-free medium. The cells then were incubated with doxorubicin for 1 h in $NaHCO_3$-free, HEPES-containing Dulbecco's medium, pH 7.4 at 37°C. After incubation, for all three cell lines, the medium (plus doxorubicin) was carefully washed out with PBS (lacking glucose to prevent drug efflux) and a coverslip was mounted carefully on the cells.

For the cell lines under study, the doxorubicin concentrations used are in the range of 2–32 μM doxorubicin, depending on the experimental set-up (for details, see Results).

Image Acquisition

For recording the images, the Zeiss Laser Scan Microscope 41 (Carl-Zeiss, Oberkochen, Germany) was used. It was equipped with an Ar and He/Ne laser, providing a 488 nm laser beam using an Argon laser or a 633 nm laser beam using the Helium/Neon laser (13). In the present study, the fluorescence images (showing doxorubicin localization in the cell) were obtained with a wavelength of 488 nm, close to the excitation maximum of doxorubicin. Detection of emission occurred at wavelengths longer than 515 nm. The images were recorded with a 2.5 mW laser intensity. The effect of the laser intensity on the fluorescence distribution was examined.

Choice of the optical magnification also was studied. With a high optical magnification, many images have to be analysed to achieve reliable results, which is time-consuming and in turn may be accompanied by unwanted changes in the fluorescence patterns in the unfixed cells, which still have to be recorded. Low optical magnification provides a larger number of cells per image but may cause an unacceptable loss of image detail and accuracy. In practice, a satisfactory optimum was obtained using a 63× antiflex Neofluar objective (oil immersion) with a N.A. of 1.25 (Carl Zeiss, Oberkochen, Germany), which corresponds to a pixel-to-pixel distance of 0.3 μm at cellular level (zoom-factor 10).

After optimizing the contrast and brightness in the fluorescence image and averaging each pixel ($n = 16$) to reduce the noise (scanning-time about 90 s), the recorded images (500 × 500 pixels, digitized to 8 bits per pixel) were transferred to a Kontron Image Processing System (IPS, Kontron Bildanalyse GmbH, Eching, Germany). Absorption images of the identical microscope fields also were sent to the Image Processing System (Fig. 1b,c).

For each image-pair (one fluorescence and one absorption image), the individual cells were magnified with a factor 2 to facilitate delineation of nucleus and cytoplasm to improve its accuracy (see Results for details).

Interactive Measurements

The doxorubicin fluorescence distribution was quantified by interactive delineation of the nucleus and the cytoplasm of the cell. For delineation of these cell com-

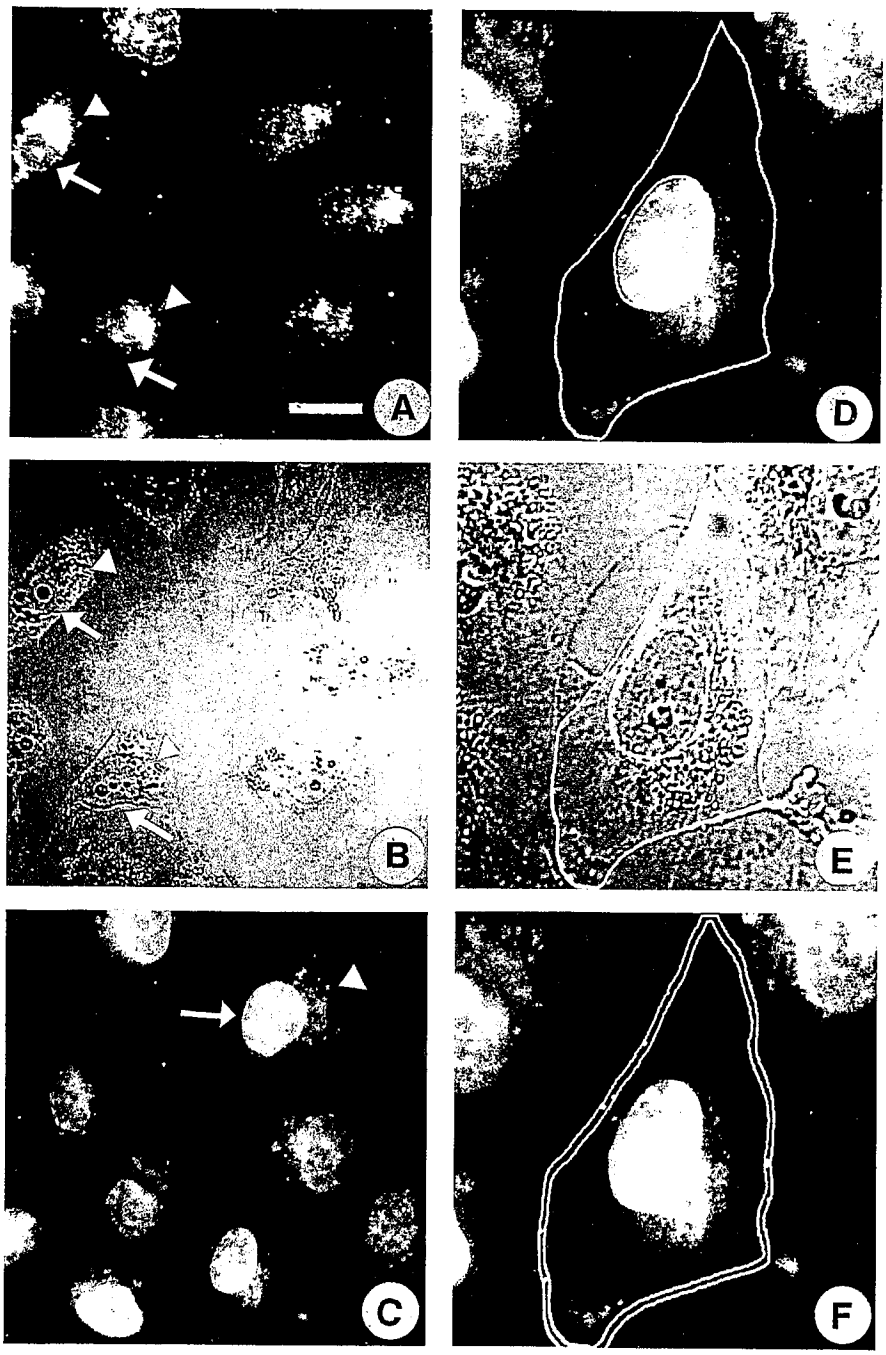

FIG. 1. Doxorubicin fluorescence distribution in SW-1573 cells and SW-1573/2R160 cells. The cells were incubated for 1 h with 6 μM doxorubicin (SW-1573) or 20 μM doxorubicin (SW-1573/2R160) at 37°C in HEPES-containing Dulbecco's medium and recorded with the laser scan microscope either in the fluorescent or in the absorption mode. Bar in A indicates 20 μm in A,B,C and 10 μm in D,E,F. Arrows and arrowheads indicate position of nucleus and cytoplasm, respectively. **A.** Doxorubicin fluorescence distribution in highly resistant SW-1573/2R160 cells. **B.** The corresponding absorption image of A. **C.** Doxorubicin fluorescence distribution in sensitive SW-1573 cells. **D.** Delineation of nucleus and cytoplasm in the fluorescence image, after magnification with a factor 2 of a cell from B. **E.** As D, but in the absorption image. **F.** Outlining of the local background area for which the calculated fluorescence values will be corrected.

partments, both the fluorescence image and the absorption image were used (Fig. 1d,e). The integrated fluorescence of the outlined regions (indicated by transmission) was computed and corrected for the intensity of the local background, which is largely due to the adjustment of brightness in the image. This background intensity was computed by defining a region, determined by a 10-fold dilation (8-connected) of the total cell area, and then excluding the cell area. This region was used as a mask in the fluorescence image to calculate the mean local background intensity, excluding the higher intensities of neighbouring cells (Fig. 1f).

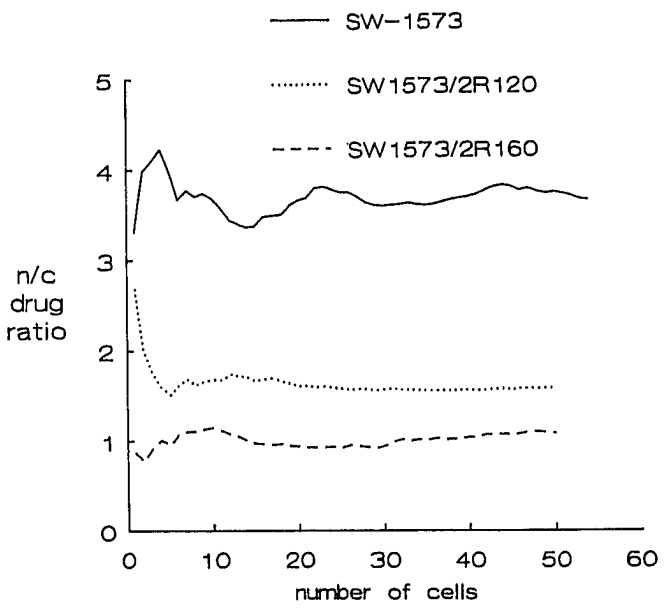

FIG. 2. The progressive mean of the N/C ratio of the SW-1573, the SW-1573/2R120, and the SW-1573/2R160 cell line. Cells were incubated for 1 h with 4 μm doxorubicin (SW-1573), and 8 μM doxorubicin (SW-1573/2R120 and SW-1573/2R160) at 37°C.

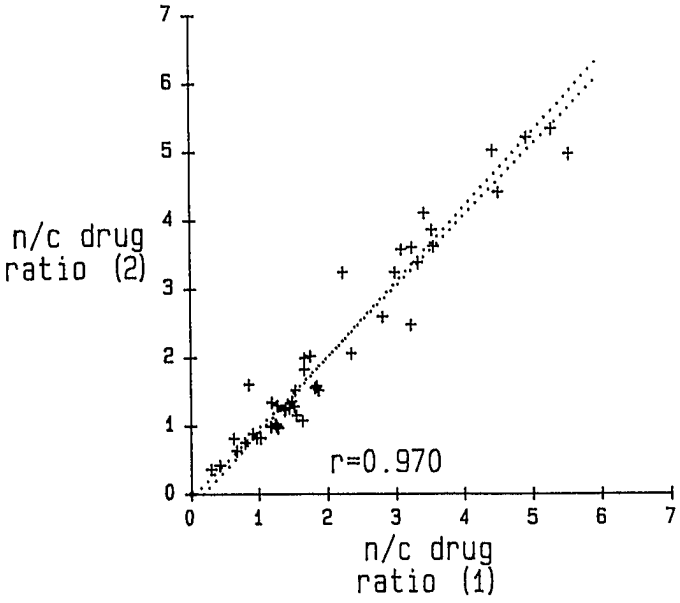

FIG. 3. The interobserver reproducibility of the interactive delineation. The N/C ratio is assessed by two observers in 15 SW-1573, 15 SW-1573/2R120, and 15 SW-1573/2R160 cells. The correlation coefficient is r = 0.970, and the slope of the best linear fit ranges between 0.91 and 1.03.

The nuclear and cytoplasmic fluorescence, from which the local background intensity was subtracted, was used to compute the fluorescence ratio of the drug in the two cell compartments from:

$$n/c\ drug\ fluorescence\ ratio = \frac{\sum_i^{n1} (I_i - \bar{I}_o)\ nucleus}{\sum_j^{n2} (I_j - \bar{I}_o)\ cytoplasm}$$

n_1, n_2 = number of nuclear and cytoplasmic pixels, respectively
I_i, I_j = intensity of nuclear and cytoplasmic pixels, respectively
I_o = mean intensity of the local background

Statistical Analysis

For evaluation of the image processing method, all analyses were performed with the BMDP statistical software package (5). In order to examine the reproducibility of the delineation, linear regression analysis was used (program P6D of BMDP). The discriminative power of the N/C ratios was investigated by the nonparametric Mann-Whitney test (program P3S).

RESULTS

First, for evaluation of the image processing method, several aspects of image acquisition, such as the laser intensity and the magnification, were investigated. Second, the results of the method were evaluated with respect to sample size, reproducibility of the interactive measurements, and detection of different levels of resistance.

Laser Intensity

The high intensity of the laser beam used to record the images may affect either the fluorescence of or the interaction of doxorubicin with its binding sites in living cells. In order to investigate the influence of the laser intensity on the fluorescence distribution, highly resistant SW-1573/2R160 cells and sensitive SW-1573 cells, for which the normal doxorubicin distribution is shown in Figure 1a and bc, respectively, were used. The standard intensity of the laser beam (5.0 mW) caused a shift of nuclear drug to the cytoplasm in the sensitive SW-1573 cells within less than 2 min exposure, which is about the time needed to record an image. When the same cells were recorded with a reduced laser intensity (2.5 mW), this phenomenon did not occur in less than 4 min. Using a 10-fold reduced laser intensity (0.5 mW), the shift did not occur, but the intensity of doxorubicin fluorescence was too low to be quantified accurately. All the laser intensities used did not affect the fluorescence distribution in the SW-1573/2R160 cells, most likely because most of the fluorescence in these cells was already present in the cytoplasm. Consequently, for all cells the 0.5 mW laser beam was used for searching representative images in the absorption mode and setting the focus level in the fluorescent mode, whereas the 2.5 mW laser beam was used for the subsequent recording of the images, which occurs in less time than needed to cause the laser-induced drug redistribution (see above).

Postmagnification

The influence of the postmagnification operation of the individual cells on the nuclear/cytoplasmic doxoru-

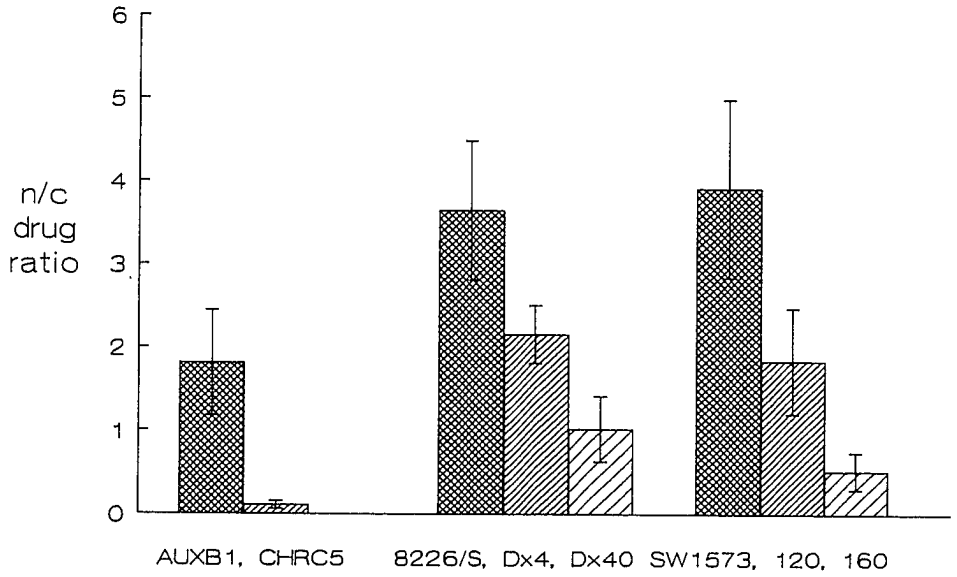

FIG. 4. N/C ratios in multidrug resistant and sensitive cells. Each bar is the mean (with standard deviation) of two independent experiments in which the number of analysed cells is 30 at minimum. The cells were incubated with doxorubicin at 37°C for 2 h with 2 μM (AUXB1), 20 μM (CH^RC5), 4 μM (SW-1573) or 8 μM (SW-1573/2R120 and SW-1573/2R160, indicated as 120 and 160, respectively, or for 1 h with 8 μM (8226/S) or 11 μM (8226/Dox4 and 8226/Dox40, indicated as Dx4 and Dx40, respectively). The N/C ratios of the cell lines with high (CH^RC_5, SW-1573/2R160 and 9226/Dox40) and low (SW-1573/2R120 and 8226/Dox4) resistance factors are significantly different from their parent (AUXB1, SW-1573 and 8226S) cell lines (Mann-Whitney; $p < 0.0001$).

bicin fluorescence ratio (N/C ratio) was investigated using at least 20 SW-1573, SW-1573/2R120 or SW-1573/2R160 cells. No significant changes in the N/C ratios were found due to this operation (Wilcoxon: $p > 0.43$). Therefore, this postmagnification procedure can be used to facilitate the delineation of the nucleus and cytoplasm.

Doxorubicin Concentration

In order to investigate whether the results were dependent on the concentration of doxorubicin, N/C ratios of SW-1573/2R120 cells, incubated with six different doxorubicin concentrations in a range of 1–32 μM doxorubicin, were measured. For these doxorubicin concentrations, the N/C ratios ratios per treatment (number of analysed cells: 40–70) ranged between 1.52 and 1.68 and were in no case significantly different from one another (Mann-Whitney: $p > 0.30$). Similar results were found for the Chinese hamster ovarian cell lines and the human myeloma cell lines (data not shown). Based on these observations, the doxorubicin concentrations were chosen such that: (1) about equal intracellular drug amounts in sensitive and resistant cells (as measured independently with radio-labelled doxorubicin, see (11)) were obtained; and (2) the signal of the doxorubicin fluorescence in each cell compartment was at least two times higher than the noise in the image.

Number of Cells

In order to obtain information about a minimal sample size, N/C ratios of SW-1573, SW-1573/2R120, and SW-1573/2R160 cells, each with a different pattern of drug distribution, were measured. For this purpose the variation of the progressive mean of the N/C ratio was investigated (Fig. 2). For each cell line the mean N/C ratio after analyzing 30 cells showed to be constant (less then 5% different from the mean N/C ratio found when more than 50 cells were analysed). These results have been confirmed for the other cell lines used in this study. Therefore, it can be concluded that a minimal sample size of 30 cells will provide reliable results.

Reproducibility of Interactive Delineation

The subjective character of the interactive delineation of the nucleus and cytoplasm may affect the results. In order to examine this, images of the human squamous lung cancer cell lines SW-1573, SW-1573/2R120, and SW-1573/2R160 were analysed. For each cell line, 15 cells were randomly selected and measured by two different observers. The correlation of the first and second assessment is 0.970 ($p < 0.001$) and the slope of the best linear fit ranges between 0.91 and 1.03 (Fig. 3).

Detection of Different Levels of Resistance

One of the major challenges of the method described in this study is to detect different (especially low) levels of doxorubicin resistance in MDR cell lines. The results of experiments with the Chinese hamster ovarian cell lines (AUXB1 and CH^RC5), the human squamous lung cancer cell lines (SW-1573, SW-1573/2R120, SW-1573/2R160), and the human myeloma cell lines (8226/S, 8226/Dox4, and 8226/Dox40) are shown in Figure 4.

The N/C ratios of the sensitive cell lines, AUXB1, SW-1573 and 8226/S, differed significantly (Mann-Whitney > 306; $p < 0.0001$) from those of cells with high (CH^RC5, resistance factor 350) or intermediate (SW-1573/2R160 and 8226/Dox40, resistance factor 45 and 50, respectively) levels of resistance. In addition, the N/C ratio shows discriminating power in distinguishing the sensitive cell lines SW-1573 and 8226/S from the cell lines SW-1573/2R120 and 8226/Dox4 (Mann-Whitney > 829; $p < 0.0001$) for which the resistance factors for doxorubicin were lower (11 and 8, respectively).

DISCUSSION

The objectives of this study were first, to investigate both the possibility and the reliability of quantification of intracellular doxorubicin fluorescence distribution in tumor cells by laser scan microscopy and digital image processing and, second, to determine which levels of resistance are detectable using this method.

The results turned out to be independent of the external doxorubicin concentrations in a range of concentrations normally used to study doxorubicin fluorescence in a quantitative way (1–32 μM). This is of particular advantage for application to patient tumor cells, for which doxorubicin concentrations have to be chosen without knowledge of total cellular drug accumulation.

It should be noted that the doxorubicin fluorescence ratios do not represent the ratios of the actual amount of the drug in the cell compartments, because the doxorubicin fluorescence is partly quenched in the nucleus (3). However, this phenomenon takes place to the same relative extent in both sensitive and resistant cells (unpublished results), and therefore, changes in N/C ratio reflect true changes in drug distribution.

One of the major advantages of this method is the low number of cells ($n = 30$) required to obtain reliable results and to give significant differences between sensitive cells and cells with low levels of resistance ($p < 0.0001$). This contrasts to other methods in which large numbers of tumor cells have to be used (summarized in (2)).

In this study, the image processing method has been tested on three cell lines, but is applicable to cell lines of other origin as well as to patient material. In addition, it will also be possible to evaluate quantitatively on such material the effect of resistance modifying agents like verapamil or bepridil, which are known to change the intracellular drug distribution (8,11,12,14). Further, it is in principle possible to stain the recorded cells afterwards with MDR-specific probes, thus enabling a combination of functional and immunocytochemical assays for a better detection of MDR (2).

For the cell lines under study, the interobserver reproducibility of the interactive delineation was high ($r = 0.970$). This interactive delineation part of the method is relatively time-consuming (1 h for 30 cells) and requires a constant precision. Currently a more automated image processing technique is in development that may reduce the time required and improve the objectivity of the measurements.

ACKNOWLEDGMENTS

The authors thank Dr. V. Ling (Ontario, Canada) for supplying the Chinese hamster ovarian cell line AUXB1 and its colchicine-resistant subline CH^RC5, Dr. W.S. Dalton (Tuscon, AZ) for supplying the human myeloma 8226 cell lines, and Dr. H. Joenje for his gift of SW-1573 cells from which the SW-1573/2R120 and SW-1573/2R160 cell were derived. The authors also thank J. van Veldhuisen for preparation of the photographs.

LITERATURE CITED

1. Baak JPA, Thunnissen FBJM, Oudejans CBM, Schipper NW: Potential uses of laser scan microscopy. J Appl Optics 26:3413–3416, 1987.
2. Broxterman HJ, Schuurhuis GJ, Lankelma J, Baak JPA, and Pinedo HM: Towards functional screening for multidrug resistant cells in human malignancies. Pezcoller Foundation Symphosia 1. Drug Resistance: Mechanisms and Reversal, Mihich, E (ed). John Libbey CIC, Romae, 1990, pp 309–319.
3. Chaires, JB, Dattagupta N and Crothers DM: Studies on interaction of anthracycline antibiotics and deoxyribonucleic acid: Equilibrium binding studies on interaction of daunomycin with deoxyribonucleic acid. Biochemistry 21:3933–3940, 1982.
4. Dalton WS, Durie BG, Alberts DS, Gerlach JH, Cress AE: Characterization of a new drug-resistant human myeloma cell line that expresses P-glycoprotein. Cancer Res 46:5125–5130, 1986.
5. Dixon WJ, ed: BMDP Biomedical computer programs. University of California Press, Berkeley, 1983.
6. Hindenburg, AA, Baker MA, Gleyzer E, Stewart VJ, Case N, Taub RN: Effect of verapamil and other agents on the distribution of anthracyclines and on reversal of drug resistance. Cancer Res 47:1421–1425, 1987.
7. Kartner N, Ling V: Multidrug resistance in cancer. Sci Am 260: 26–33, 1989.
8. Keizer HG, Schuurhuis GJ, Broxterman HJ, Lankelma J, Schoonen WG, van Rijn J, Pinedo HM, Joenje H: Correlation of multidrug resistance with decreased drug accumulation, altered subcellular drug distribution, and increased P-glycoprotein expression in cultured SW-1573 human lung tumor cells. Cancer Res 49:2988–2993, 1989.
9. Kuiper CM, Broxterman HJ, Baas F, Schuurhuis GJ, Haisma HJ, Scheffer GL, Lankelma J, Pinedo HM: Drug transport variants without P-Glycoprotein overexpression from a human squamous lung cancer cell line after selection with doxorubicin. J Cell Pharmacol (in press).
10. Ling V, Thompson LH. Reduced permeability in CHO cells as a mechanism of resistance to colchicine. J Cell Physiol 83:103–116, 1974.
11. Schuurhuis GJ, Broxterman HJ, Cervantes A, van Heijningen THM, de Lange JHM, Baak JPA, Pinedo HM, Lankelma J. Quantitative determination of factors contributing to doxorubicin resistance in multidrug-resistant cells. J Natl Cancer Inst 81:1887–1892, 1989.
12. Schuurhuis GJ, Broxterman HJ, van der Hoeven JJM, Pinedo HM, Lankelma J. Potentiation of doxorubicin cytotoxicity by the calcium antagonist bepridil in anthracycline-resistant and -sensitive cell lines. Cancer Chemother Pharmacol 20:285–290, 1987.
13. Wilke V. Optical Scanning Microscopy: The Laser Scan Microscope. Scanning 7:88–96, 1985.
14. Willingham, MC, Cornwell MM, Cardarelli CO, Gottesmann MM and Pastan I. Single cell analysis of daunomycin uptake and efflux in multidrug-resistant and -sensitive KB cells: Effects of verapamil and other drugs. Cancer Res 46:5941–5946, 1986.